CHAPTER VI
DIELECTRIC PROPERTIES OF BARIUM STRONTIUM TITANATE/ POLYBENZOXAZINE COMPOSITE WITH 0-3 CONNECTIVITY

6.1 Abstract

Polymer-ceramic composites with 0-3 connectivity were fabricated from barium strontium titanate ($Ba_{0.7}Sr_{0.3}TiO_3$) and polybenzoxazine. Effects of ceramic content, temperature and frequency on the dielectric properties of composites were discussed. The $Ba_{0.7}Sr_{0.3}TiO_3$ ceramic powders were prepared by sol-gel method. The amount of sol-gel $Ba_{0.7}Sr_{0.3}TiO_3$ powders (SG-BST) in polybenzoxazine matrix was varied from 30 – 80 wt% in order to investigate the effect of ceramic contents on dielectric behavior of the composites. It was found that the dielectric constant of composites increased with increasing ceramic contents. By adding 80 wt% (48 vol%) of ceramic fillers, the dielectric constant was as high as 28. The dielectric constants of the composites are nearly stable with frequency range of 1 kHz – 10 MHz and temperature range of 20-130°C. Loss tangent of these composites are less than 0.05. The measured dielectric constant was fitted well with Yamada model indicating 0-3 connectivity.

Keywords: Polybenzoxazine, Barium strontium titanate, Polymer-ceramic composites, Dielectric properties

6.2 Introduction

Recently, embedded capacitor technology plays an important role for the miniaturization products because of the major benefits over traditional discrete capacitors including better electrical performance, higher reliability, small size, and improved designed options. Importance requirements for embedded capacitors materials include high dielectric constant, low capacitance tolerance, good processability, and low cost. [1-4]. Materials required for the embedded capacitor should have dielectric constant of 25-170 and should be processed at low processing temperature, tough ,and flexible in order to compatible with the printed circuit board (PCB) manufacturing process. Polymer has generally low dielectric constant and it is not suitable for the capacitor requirements. On the other hand, ceramics have high dielectric constant but require high processing temperatures [5].

Polymer-ceramic composites are one of the great interest and the candidate materials for embedded capacitor application because they combine the processability of the polymer with high dielectric constant of the ceramics, resulting in low processing temperature and cost. Among the composites studied so far, the simplest type is 0-3 connectivity, consisting of a three-dimentionally connected polymer matrix filled with ceramic particles. This type of connectivity is easy to fabricate and suitable for mass production [6]. However, dielectric properties are dominated by properties of matrix material. In polymer-ceramic composites, polymer matrix possesses lower dielectric constant in comparison to ceramic particle. The dielectric properties of composites are strongly influenced by the ceramic phase, including content, particle size, and distribution. In addition, it can be also affected by porosity and filler distribution. In the same way, the necessary amount of filler should be enough more than 30% in volume in order to change the dielectric constant of the composites. However, these high amounts of ceramic filler may make composite processing more difficult [7].

In recent year, epoxy and polyimide are generally used for embedded capacitor because of its compatibility with PWBs and good thermal stability. Barium titanate ($BaTiO_3$), a well known ferroelectric material, is selected as filler because it has high dielectric constant and lead-free composition. $BaTiO_3$ are widely used in many electronic applications such as capacitor, transducer, phase shifter, etc. The dielectric constant of $BaTiO_3$ is around 6000 for a fine grain size of ~1 μm, and of 1500-2000 at a coarse grain size [8, 9]. The dielectric constant of $BaTiO_3$ at Curie point has the highest value of 10000 but decrease as increasing temperature. The strontium (Sr^{2+}) is used to dope in $BaTiO_3$ by substituting in Ba^{2+} in order to shift the Curie peak toward to room temperature, which can improve the dielectric constant [10, 11]. Fu *et al.* reported that Curie peak shift to near room temperature by doping strontium molar concentration of 0.35 [12]. The dielectric properties of $BaTiO_3$ ceramics are strongly related to the grain size and the type of dopant used. In polymer-ceramic composite system, the $BaTiO_3$ is in the powder form instead of the sintered form. The behaviors of $BaTiO_3$ powder is also related to the particle size, phase content and the dopants. The decrease in particle size results in the removal of grain boundaries, elimination of constrained forces from neighboring grains and a drop in domain density, which result in the decrease in dielectric constant of $BaTiO_3$ powder. As particle sizes increase, unsintered powder become a ceramic-like body and possesses similar properties as ceramics. Therefore, the unsintered powders and sintered ceramics of $BaTiO_3$ are different in the dielectric behaviors depending on the particle size.

To prepare ceramic powders, sol-gel method offers significant advantage in obtaining the powder with high impurity and homogeneous, through a lower temperature process, avoiding contamination of materials [13]. In this study, polybenzoxazine thermosetting resins have been proposed as polymer matrix because they were found to possess several outstanding properties such as near–zero shrinkage after curing, high thermal stability, and flexibility in molecular design [14].

The sol-gel $Ba_{0.7}Sr_{0.3}TiO_3$ powders (SG-BST) was used as ceramic filler incorporating in polybenzoxazine matrix. The dielectric properties of SG-BST/polybenzoxazine composites as function of ceramic content, frequency, and temperature were measured and discussed. These composites were fabricated in bulk pellet form by compression molding. Moreover, the effect of ceramic content on the dielectric properties of composites can be explained and predicted by various theoretical mixing models, including Yamada model [15], Bruggeman formulae [16], Lichtenecker model [16], and Kerner expression modified by Jayasundere-Smith [17].

6.3 Experimental

6.3.1 Synthesis of Benzoxazine

The synthesis of benzoxazine is based on the reaction of phenol, paraformaldehyde, and ethylenediamine at the molar ratio of 2:4:1 respectively.

Solution of paraformaldehyde and ethylenediamine in chloroform was stirred for 30 min in ice bath. Phenol chloroform solution was then added and stirred for 30 min. The mixture was refluxed at temperature of 60°C for 1 h followed by evaporating chloroform out. High yellow viscous solution was obtained, and dissolved it in diethyl ether. The ether solution was washed with 2N NaOH solution in separatory funnel. The ether was removed with a rotary evaporator, and the solid products were washed by cool methanol to obtain white benzoxazine powders. Network structure of a linear aliphatic diamine-based polybenzoxazine are polymerized by ring opening polymerization and initiated by heat, as shown in Figure 6.1 [18].

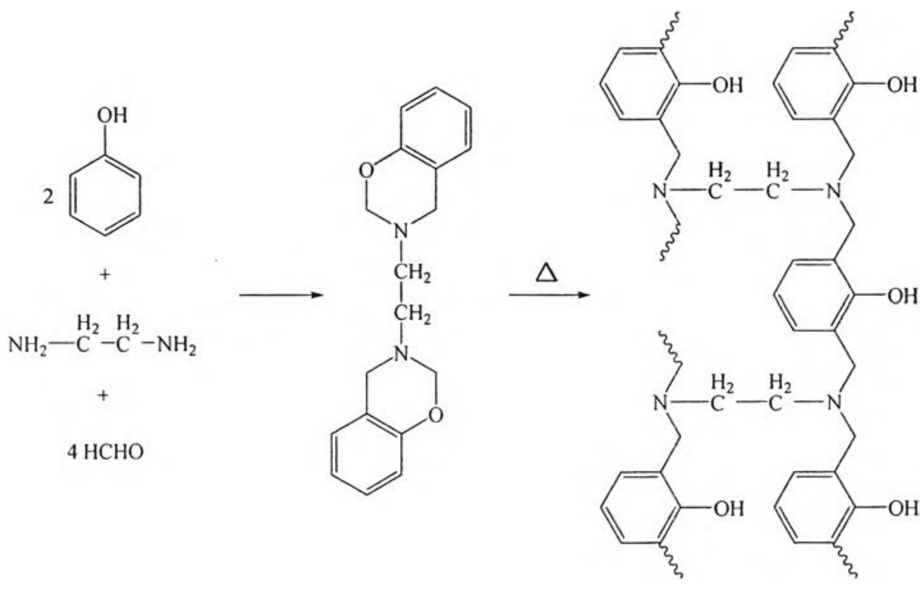

Figure 6.1 Synthesis and thermal polymerization of benzoxazine.

6.3.2 Preparation of Barium Strontium Ttitanate

For preparation of sol-gel precursor gel, barium acetate [$Ba(CH_3COO)_2$, purity > 99%, Aldrich], strontium acetate [$Sr(CH_3COO)_2$, purity > 99%, Fluka], and titanium (iv)n-butoxide [$Ti(O(CH)_3CH_3)_4$, Aldrich] were used as starting materials. Gracial acetic acid [CH_3COOH, Labscan] and methanol [CH_3OH, Labscan] were used as solvent. The proper amounts of the barium acetate and strontium acetate were firstly dissolved in heat acetic acid with stirring to obtain clear solution followed by adding methanol with acetic acid: methanol ($R_{ac/me}$) of 1:2. The equimolar amount of titanium (iv) n-butoxide was then added into the mixture under vigorous stirring. The clear solution was stable and became a gel in a few days. The gels were calcined by using 2-step thermal decomposition at 500 and 800°C in order to decompose the solvent and crystallize the barium strontium titanate (Figure 3.1). Afterward, the sol-gel $Ba_{0.7}Sr_{0.3}TiO_3$ powders were pressed into disks shape, and then sintered at the temperature of 1350°C for 2 h (Figure 3.2) in order to measure dielectric properties.

6.3.3 Fabrication of Polymer-Ceramic Composites

The polybenzoxazine before curing was in the powder form. Thus the ceramic powders and benzoxazine powders could be homogeneously blended by the dry mixing method (mechanically grinding in pestle moltar), with 30, 40, 50, 60, 70, and 80 wt%. The composite specimens were prepared by compression molding, and cured at 120, 140, 160°C for 30 min, then for further 1 h at 180°C under pressure of 10 metric tones (Table 3.1). The disk shape composite specimens of 15 mm diameter and 1 mm diameter were fabricated, and used for further measurements and characterizations.

6.3.4 Characterizations

Fourier transforms infrared spectra (FTIR) of benzoxazine were obtained using a Nicolet NEXUS 670 system. Thermo gravimetric analysis (TGA) was performed using a TG-DTA Pyris Diamond (Perkin Elmer). The mass change with increasing temperature was monitored and recorded from 50°C to 900°C with a heating rate of 10°C/min under N_2 flow. The melting temperature of benzoxazine was investigated by a differential scanning calorimeter, DSC 7 (Perkin Elmer) under N_2 purge at a heating rate of 10 °C/min.

The density of polybenzoxazine, ceramic powders (SG-BST), and composites were measured by pycnometer (Quantachrome, Ultrapycnometer 1000). Crystallinity and structure of SG-BST were analyzed using X-ray diffraction (XRD, Rigaku, model Dmax 2002) with Cu Kα radiation and a Ni filter, at 40 kV and 30mA. Particle size of SG-BST, microstructure of BST ceramic, and distribution of ceramic powders in composites were observed using scanning electron microscope (SEM; JSM-6480LV, JEOL and JSM-5200, JEOL).

For dielectric measurement, the composite specimens were coated with gold sputtering as electrodes. The dielectric properties of the composites were measured using Hewlett-Packard 4194A impedance/gain phase analyzer. The dielectric measurements were performed as function of frequency (1 kHz – 10 MHz) and temperature (20-130°C). The dielectric constant of composites was calculated from the capacitance by using the following equation:

$$K = \frac{CA}{\varepsilon_0 d} \tag{6.1}$$

where C is the capacitance (F), ε_0 the free space dielectric constant value (8.85×10^{-12} F/m), A the capacitor area (m^2), and d the thickness of specimens.

6.4 Results and Discussion

6.4.1 Polybenzoxazine Characterization

The structure of the benzoxazine was examined by FTIR. The FTIR spectrums of benzoxazine are shown in Figure 6.2. The bands that appear in the frequency region 1550-1400 cm^{-1} were due to the substituted benzene ring. The bands in the region 1240-1210 cm^{-1} and 1040-1020 cm^{-1} corresponded to the asymmetric and symmetric C-O-C stretching modes. The region of 1150-1050 cm^{-1} was due to the C-N-C asymmetric stretching, while the symmetric stretching mode appeared at 800-720 cm^{-1}. Additionally, the characteristic absorption assigned to out of plane bending vibrations of C-H at 920 cm^{-1} was observed, indicating the benzoxazine ring formation [8]. For molecular weight of benzoxazine, M_n was 1242, and M_w was 1519.

The DSC thermogram in Figure 6.3 shows that peak of endotherm occurred at 105°C. It indicated that the melting temperature of benzoxazine was around 105°C. Polybenzoxazine was polymerized by ring opening polymerization, initiated by heat and curing at temperature of 180°C. The TGA thermogram of the polybenzoxazine is shown in Figure 6.4. The onset of weight loss is approximately 236°C and could be deemed as a high char yield polymer (43%) at temperature of 800°C. The decomposition temperature (T_D) of polybenzoxazine was 247°C, which was defined as the temperature with 5% of weight loss of resin when subjected in nitrogen atmosphere [14]. The properties of benzoxazine and polybenzoxazine based diamine are summarized in Table 6.1.

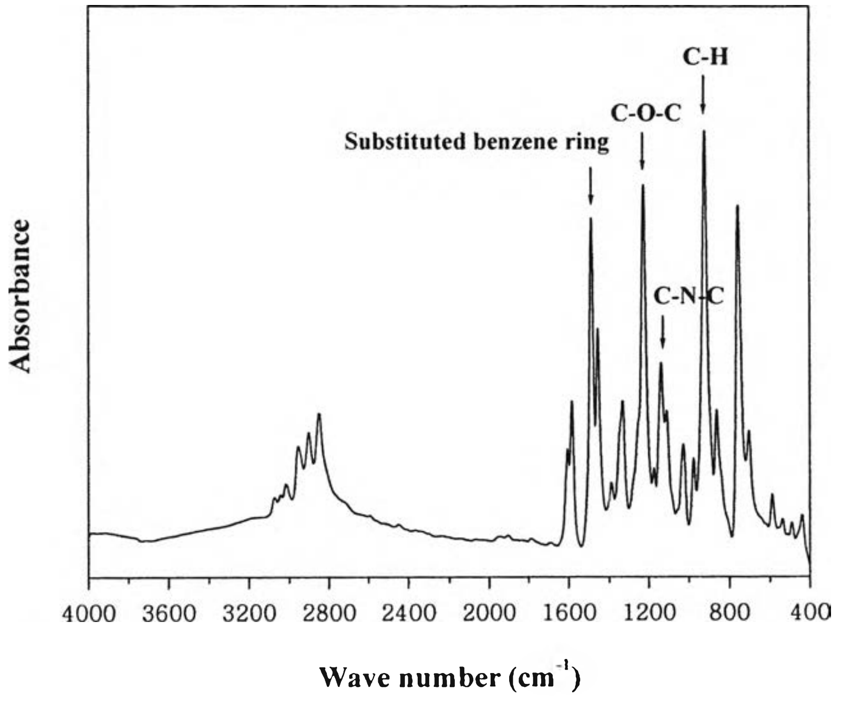

Figure 6.2 FTIR spectrum of benzoxazine based diamine.

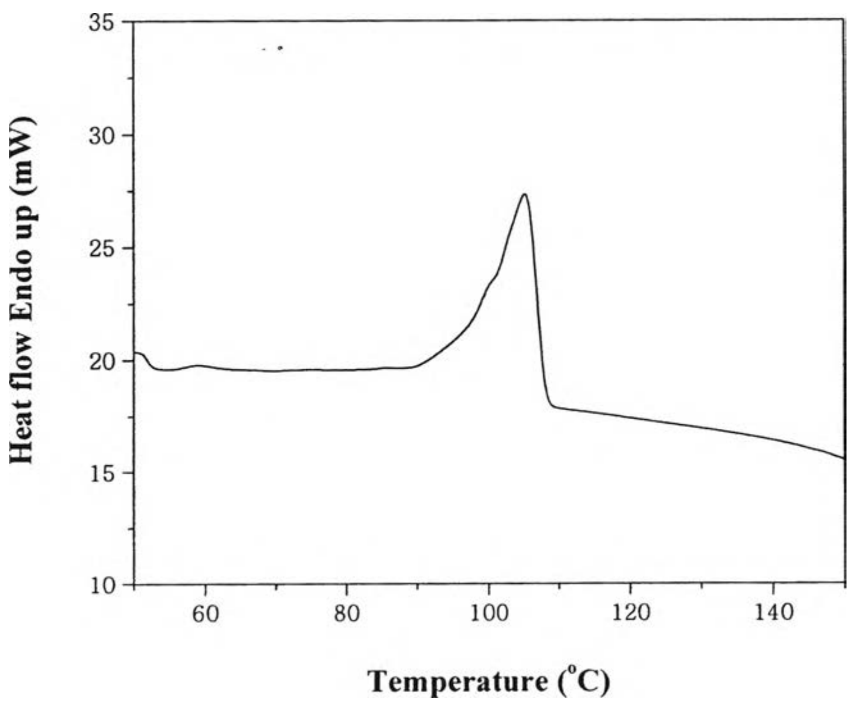

Figure 6.3 DSC thermogram of benzoxazine based diamine.

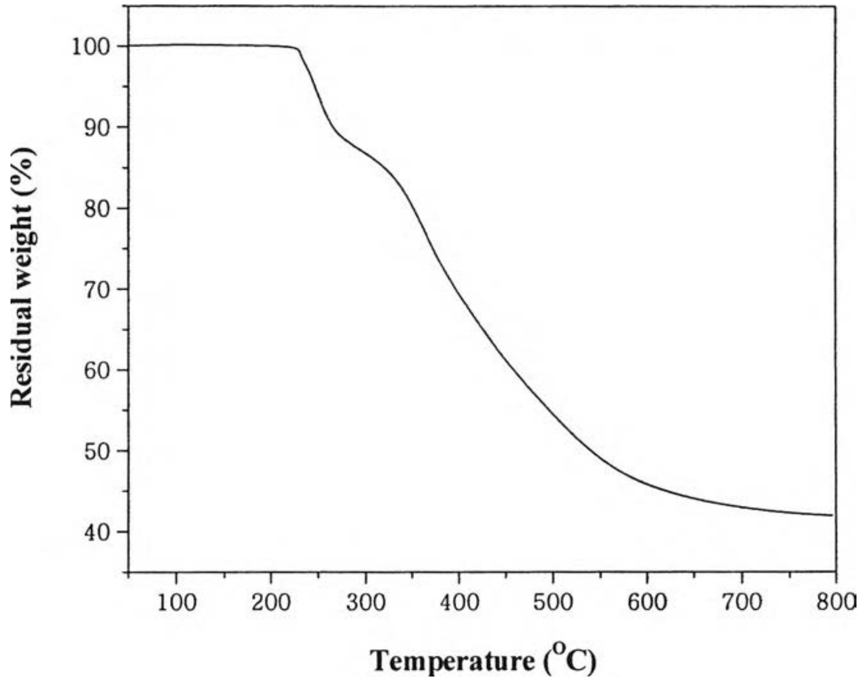

Figure 6.4 TGA curve of polybenzoxazine in nitrogen atmosphere.

Table 6.1 Properties of benzoxazine and polybenzoxazine based diamine.

Properties	Value
Density	
Benzoxazine ($x10^{-3}$ kg/m^3)	1.31
Polybezoxazine ($x10^{-3}$ kg/m^3)	1.18
Molecular weight: M_w/M_n	1519/1242
Melting temperature (°C)	105
Decomposition temperature (°C)	247
Char yield (wt%)	43
Dielectric constant (at 1 kHz)	3.81
Loss tangent (at 1 kHz)	0.017

6.4.2 Barium Strontium Titanate Characterization

The morphology of SG-BST powders after calcining at 800°C is shown by SEM micrographs in Figure 6.5(a). It shows that particles of SG-BST were in the range of 50-80 nm and narrow size distribution. Figure 6.5(b) reveals the microstructure of $Ba_{0.7}Sr_{0.3}TiO_3$ ceramic after sintering at 1350 °C for 2 h. X-ray diffraction was used to structurally characterize the crystallization of SG-BST, as shown in Figure 6.6. All characteristic peaks of SG-BST corresponded to perovskite structure in a cubic phase.

The dielectric properties of $Ba_{0.7}Sr_{0.3}TiO_3$ ceramics were measured in the frequency range of 1 kHz - 10 MHz at room temperature, as shown in Figure 6.7. As can be seen, the dielectric constant was 2795 at 1 kHz. At frequency above 1 MHz, the dielectric constant decreased rapidly and a sudden increase in dielectric loss was observed. It indicated that ceramic exhibited large dielectric relaxation at frequency greater than 1 MHz. This phenomenon was ascribed by the effect of internal stress in the grain and domain-wall motion [19, 20].

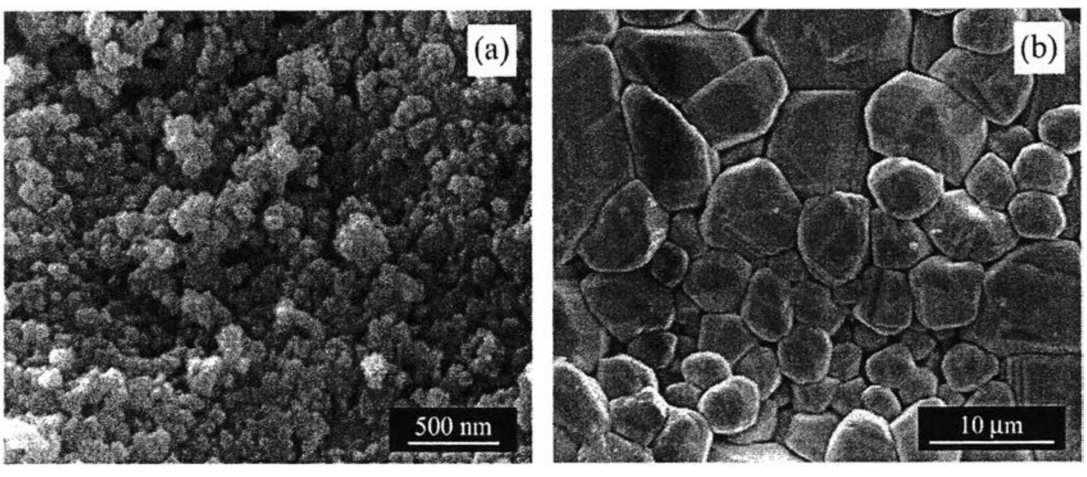

Figure 6.5 SEM micrographs; (a) sol-gel $Ba_{0.7}Sr_{0.3}TiO_3$ powders and (b) $Ba_{0.7}Sr_{0.3}TiO_3$ ceramic.

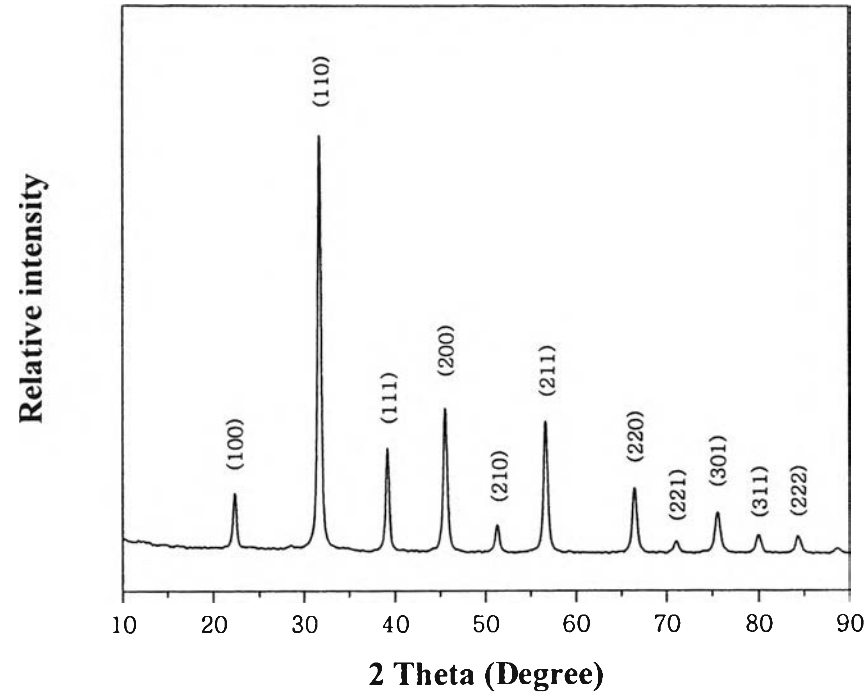

Figure 6.6 XRD pattern of sol-gel $Ba_{0.7}Sr_{0.3}TiO_3$ powders.

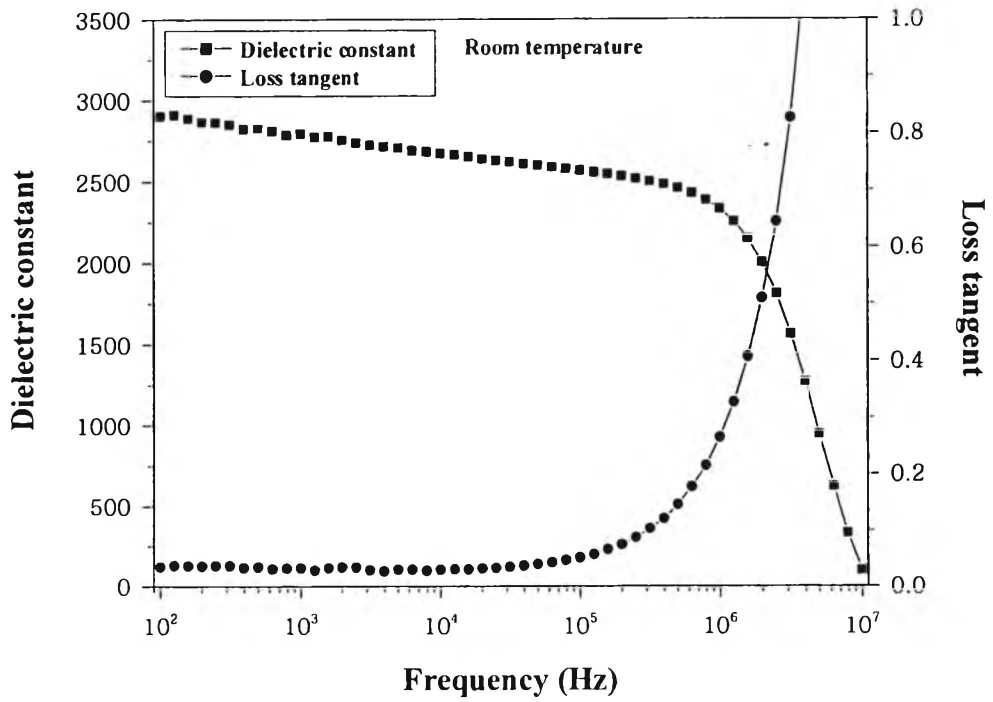

Figure 6.7 Dielectric properties as a function of frequency for $Ba_{0.7}Sr_{0.3}TiO_3$ ceramic.

6.4.3 Composite Characterization

6.4.3.1 Density Measurement

The density of the polybenzoxazine cured at 180°C for 1 h, ceramic fillers, and the composites was measured by pycnometer. Theoretical density (ρ_T) was calculated using equation (6.2)

$$\rho_T = (1-\phi)\rho_p + V\rho_c \tag{6.2}$$

where ρ_c is the filler density, ρ_p is the polymer matrix density and ϕ is the volume fraction of filler. Density of polybenzoxazine and SG-BST is 1.18 and 5.39 g/cm^3, respectively. The densities of the composites with various filler loading are summarized in Table 6.2. Figure 6.8 reveals that experimentally measured density could be fitted well with theoretical density at various ceramic contents.

The compositions of the ceramic filler in composites were also confirmed by considering residual weight of each composite, as shown in Figure 6.9. The residual weight increased with increasing the amount of ceramic fillers because the ceramic fillers do not decompose at low temperature. The filling of ceramic fillers improved the thermal stability obviously. The increase in decomposition temperature was attributed to the enhancement of interaction between the polybenzoxazine matrix and the ceramic powders, which limited the movement of polybenzoxazine.

Table 6.2 Properties of the composites at various SG-BST contents

Composites	Volume fraction	Density (g/cm^3)	Residual weight% at 800°C
PBZZ/SG-BST 30 wt%	0.10	1.81	56.37
PBZZ/SG-BST 40 wt%	0.15	1.97	61.87
PBZZ/SG-BST 50 wt%	0.20	2.11	69.00
PBZZ/SG-BST 60 wt%	0.25	2.23	74.02
PBZZ/SG-BST 70 wt%	0.38	2.88	78.78
PBZZ/SG-BST 80 wt%	0.48	3.55	83.83

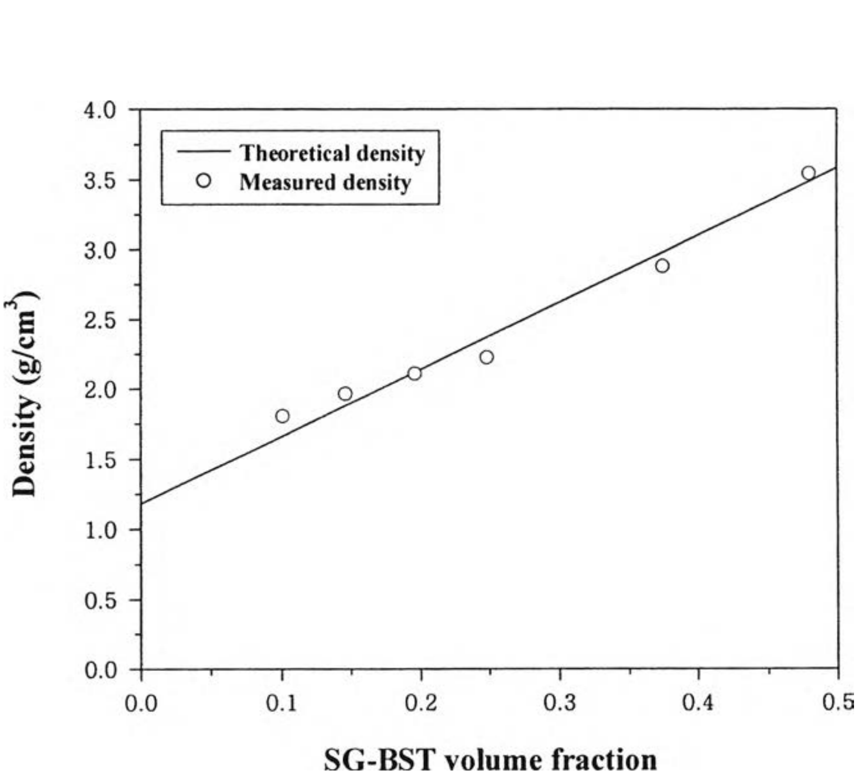

Figure 6.8 Comparison between measured density (o) and theoretical density (—) as a function of SG-BST volume fraction.

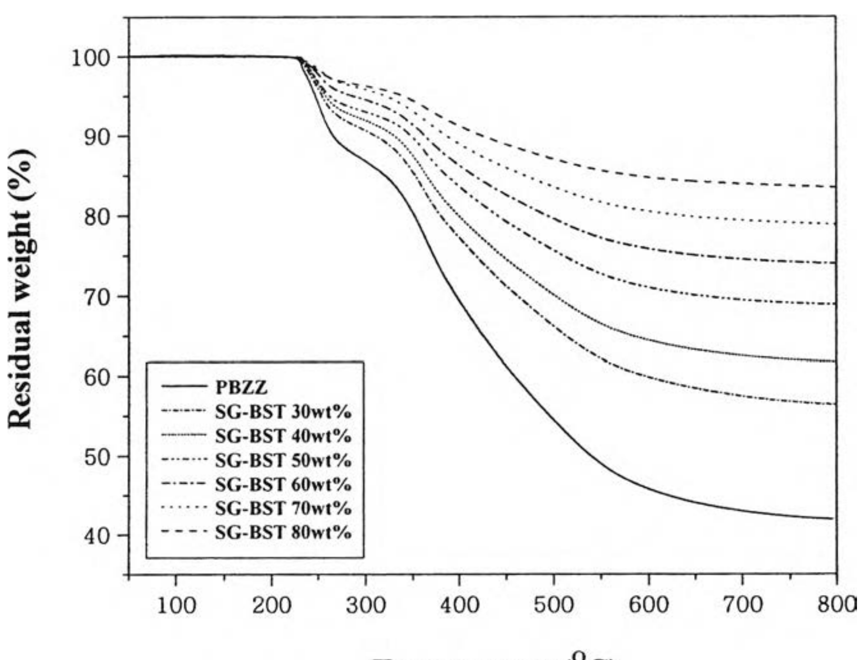

Figure 6.9 TGA curve of the composites at different SG-BST contents in nitrogen atmosphere.

6.4.3.2 Ceramic Filler Distribution

The distribution of ceramic fillers in the polybenzoxazine matrix was investigated by SEM micrographs. Figure 6.10 (a)-(f) show fracture and surface morphology of the composites with the SG-BST of 30, 50 and 70 wt%, respectively. The white and gray colors represent the ceramic fillers and the polybenzoxazine matrix, respectively. All composites with different filler content show homogeneous dispersion with small trail of agglomeration. Additionally, it could be observed that SG-BST filler tend to form larger agglomeration, which might occur due to SG-BST particles easily form agglomerates by van der waals force.

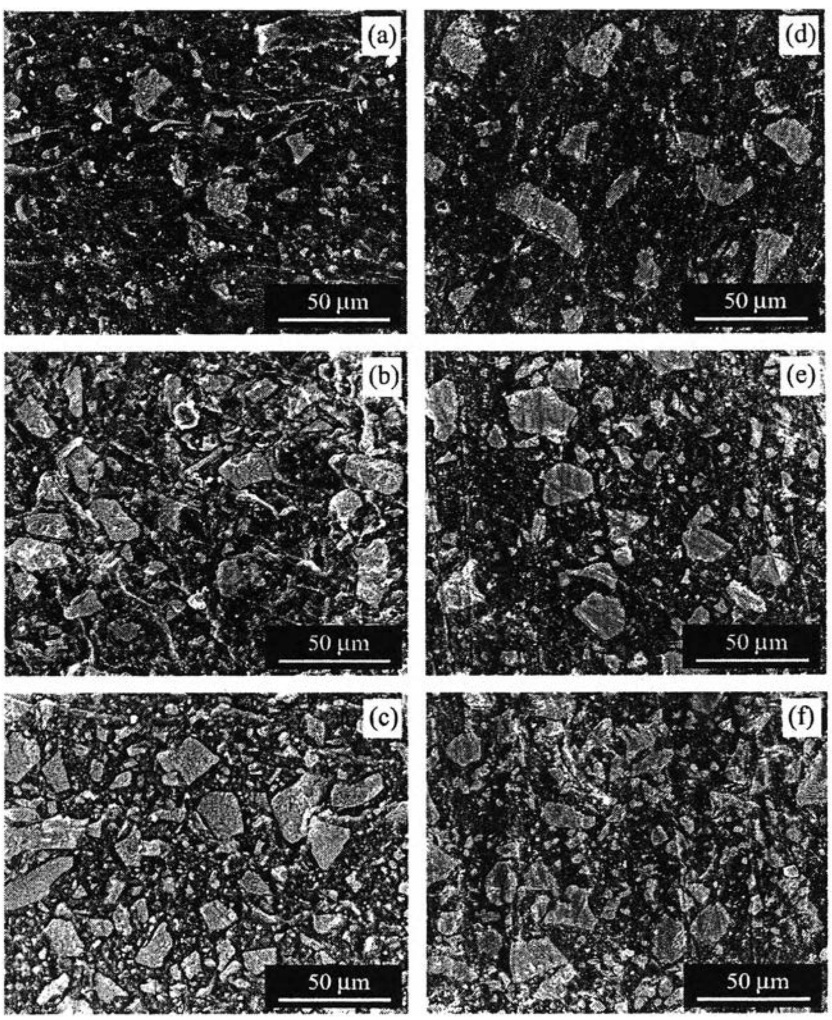

Figure 6.10 SEM micrographs of the composites: fracture morphology (a) 30 wt%, (b) 50 wt%, and (c) 70 wt%: surface morphology (d) 30 wt%, (e) 50 wt%, and (f) 70 wt%.

6.4.3.3 Dielectric Properties of Composites

As can be seen in Figure 6.11, it was found that the dielectric constant increased with increasing ceramic content. The dipole-dipole interaction increased and contributed to higher dielectric constant when ceramic filler come closer at higher filler loading. For the composites with 80 wt% (48 vol%) of SG-BST, the composite had dielectric constant as high as 28, at 1 kHz. Previously, Xie *et al.* reported the dielectric constant of polyimide/$BaTiO_3$ was 35 at 50 vol% of $BaTiO_3$ [21]. Cheng *et al.* reported the dielectric constant of the epoxy containing 80 wt% (45 vol%) of $BaTiO_3$ could be increased from 3.2 to 13.1 at frequency of 1 GHz [22]. This result could be explained by interfacial polarization inside the composites in applied alternating field.

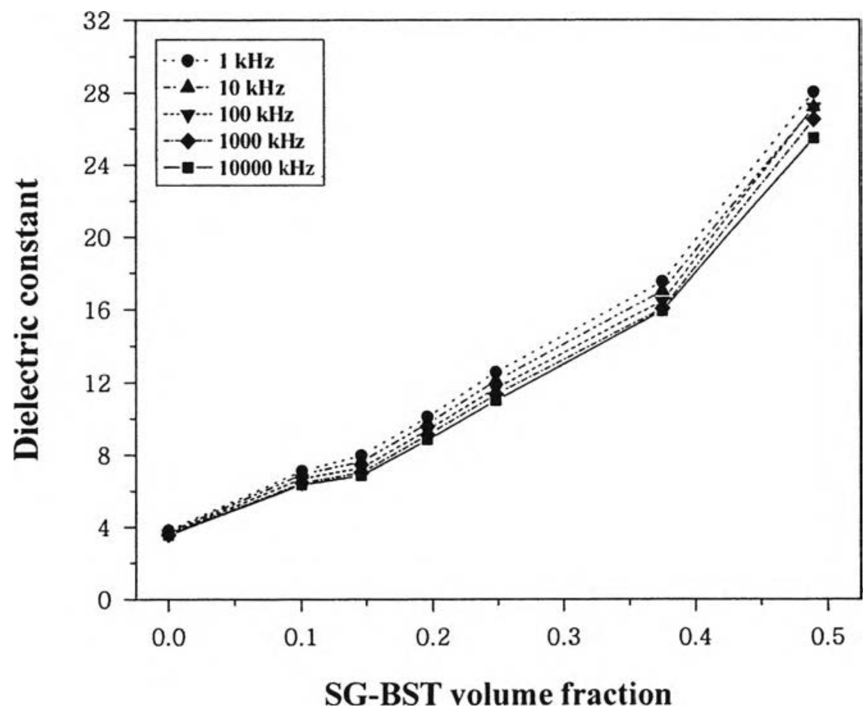

Figure 6.11 Dielectric constant of the composites at different SG-BST volume fraction and frequencies.

Figure 6.12 shows the frequency dependence of the dielectric constant with various ceramic contents. The dielectric constant slightly decreased with increasing frequency, which referred to frequency independence behavior. There are two causes of this phenomenon: (a) decreasing in dipolar polarization in polymer matrix; (b) decreasing in interfacial polarization or Maxwell Wagner-Sillar (MWS). Interfacial polarization was produced from the accumulation of charges at the interface between ceramic and polymer resulting in a large scale field distortion, which is different from the other types of polarization (atomic, electronic, dipolar), being produced by the displacement or orientation of bound charge carriers [7]. The decrease in polarization was due to the delay in molecular polarization with respect to a changing frequency in a dielectric medium. The loss tangent of the composites at various frequencies is shown in Figure 6.13. It was found that loss tangent of all composites (<0.05) was greater than pure polybenzoxazine. The loss tangent of the composites increased around three times comparing with pure polybenzoxazine. The increase of loss tangent value was due to the formation of porosity in the specimens.

Moreover, the dielectric properties of the composites were also measured as a function of temperature varying from 20-130°C at 1 MHz, which are shown in Figure 6.14-6.15. It was found that a slightly increasing tendency in dielectric constant and loss tangent were observed while the temperature increased. The composite dielectric constants of all compositions only increased less than 10%. This phenomenon could be explained that segmental mobility of polymer was improved by increasing temperature, resulting in facilitate polarization of ceramic filler and increased dielectric constant, consequently [21].

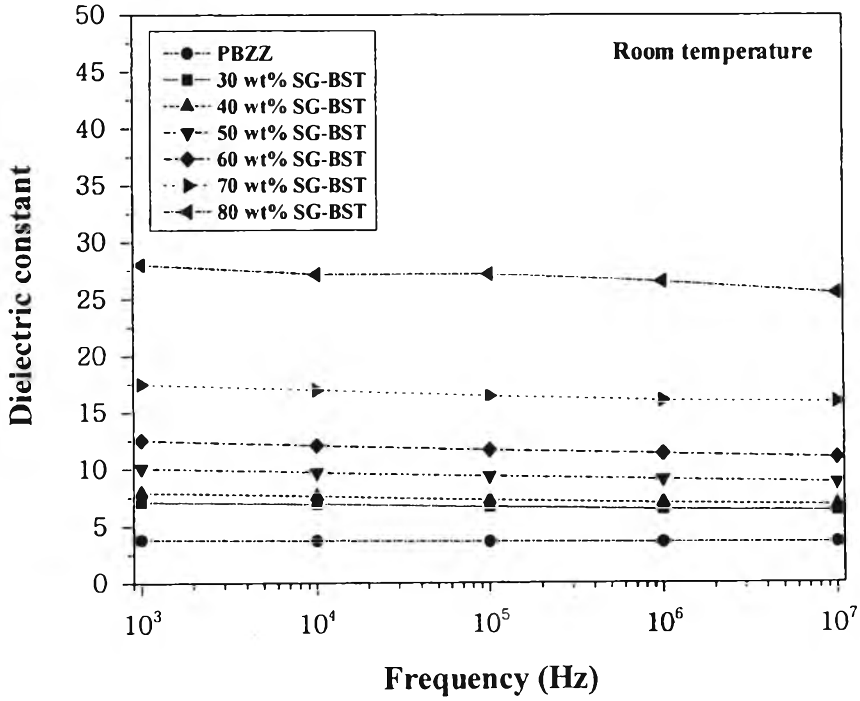

Figure 6.12 Frequency dependence of dielectric constant for the composites at various SG-BST contents.

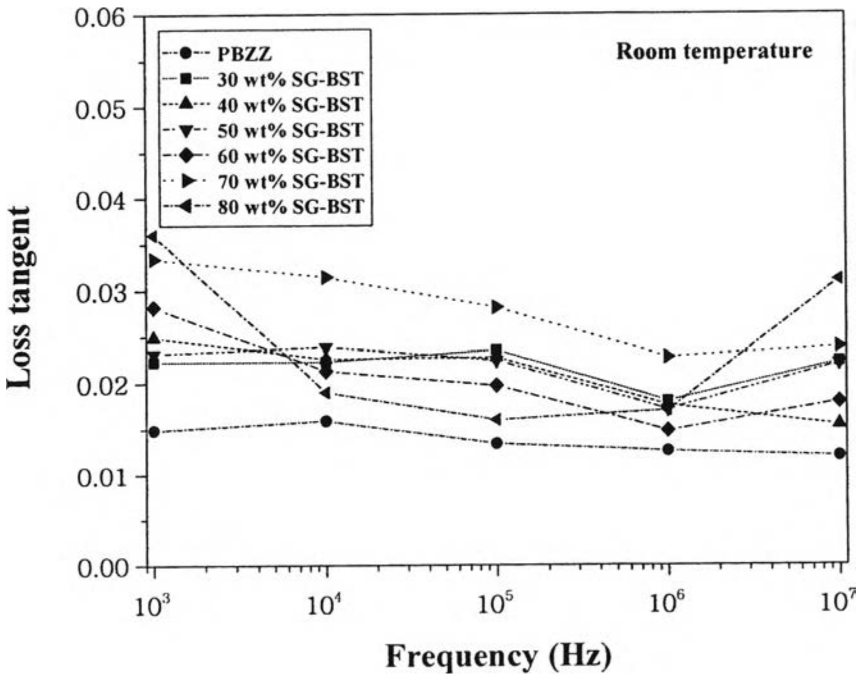

Figure 6.13 Frequency dependence of loss tangent for the composites at various SG-BST contents.

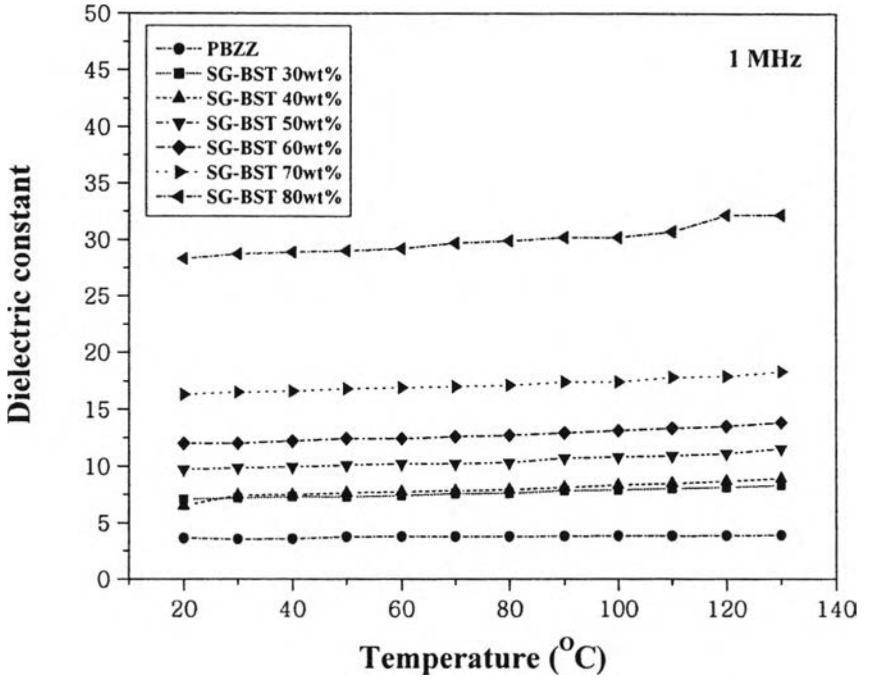

Figure 6.14 Temperature dependence of dielectric constant for the composites at various SG-BST contents.

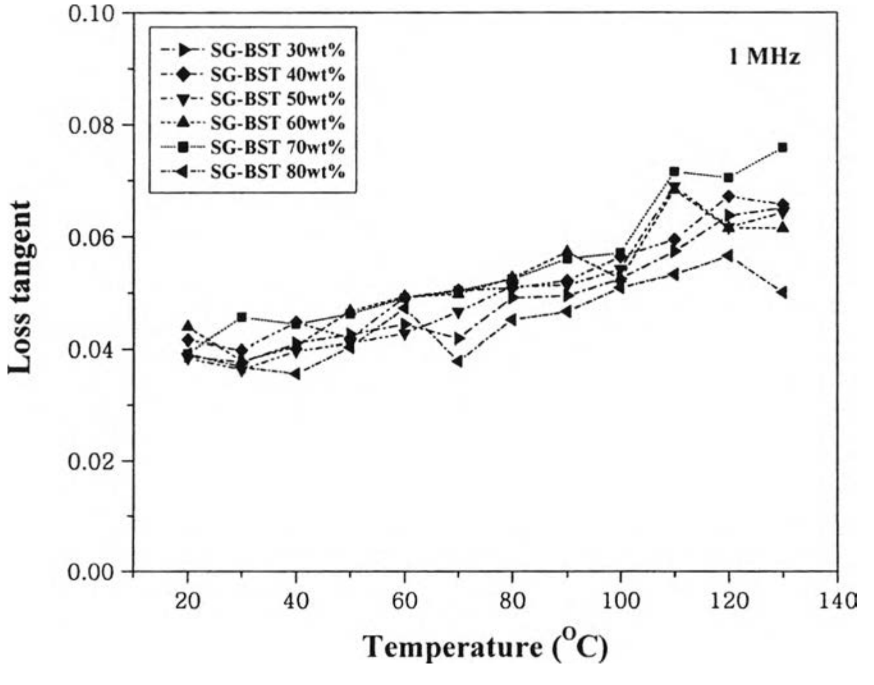

Figure 6.15 Temperature dependence of loss tangent for the composites at various SG-BST contents.

6.4.3.4 Experimeantal Data Fitting

Four theoretical mixing models for 0-3 connectivity have been proposed in order to calculate the dielectric constant of the composites comparing with experimental results, including Yamada model, Bruggeman formulae, Lichtenecker model, and Kerner expression modified by Jayasundere-Smith (J-S prediction), as shown in Figure 6.16. The equations of these models are described as follow:

Yamada model
$$\varepsilon = \varepsilon_p \left[\frac{\eta\phi(\varepsilon_c - \varepsilon_p)}{\eta\varepsilon_p + (\varepsilon_c - \varepsilon_p)(1+\phi)} \right] \tag{6.2}$$

Lichtenecker model
$$\log\varepsilon = \log\varepsilon_p + \phi\log\left(\frac{\varepsilon_c}{\varepsilon_p}\right) \tag{6.3}$$

Bruggeman formulae
$$\frac{\varepsilon_c - \varepsilon}{\varepsilon_c - \varepsilon_p}\left(\frac{\varepsilon_p}{\varepsilon}\right)^{1/3} = 1 - \phi \tag{6.4}$$

Kerner expression
$$\varepsilon = \frac{\varepsilon_p\phi_p + \varepsilon_c\phi_c[3\varepsilon_p/(\varepsilon_c + 2\varepsilon_p)][1 + 3\phi_c(\varepsilon_c - \varepsilon_p)/(\varepsilon_c + 2\varepsilon_p)]}{\phi_p + \phi_p(3\varepsilon_c)/(\varepsilon_p + 2\varepsilon_c)[1 + 3\phi_c(\varepsilon_c - \varepsilon_p)/(\varepsilon_c + 2\varepsilon_p)]} \tag{6.5}$$

where ε is the dielectric constant of the composites, ε_p and ε_c refer to the dielectric constants of the polymer matrix and the BST ceramic, respectively, ϕ is the volume fraction of ceramic and η is a shape parameter. For the calculation, the dielectric constant of $Ba_{0.7}Sr_{0.3}TiO_3$ ($\varepsilon_c = 2795$) and the pure polybenzoxazine ($\varepsilon_p = 3.81$) were used. The dielectric constants were measured at room temperature (~25°C) and 1 kHz.

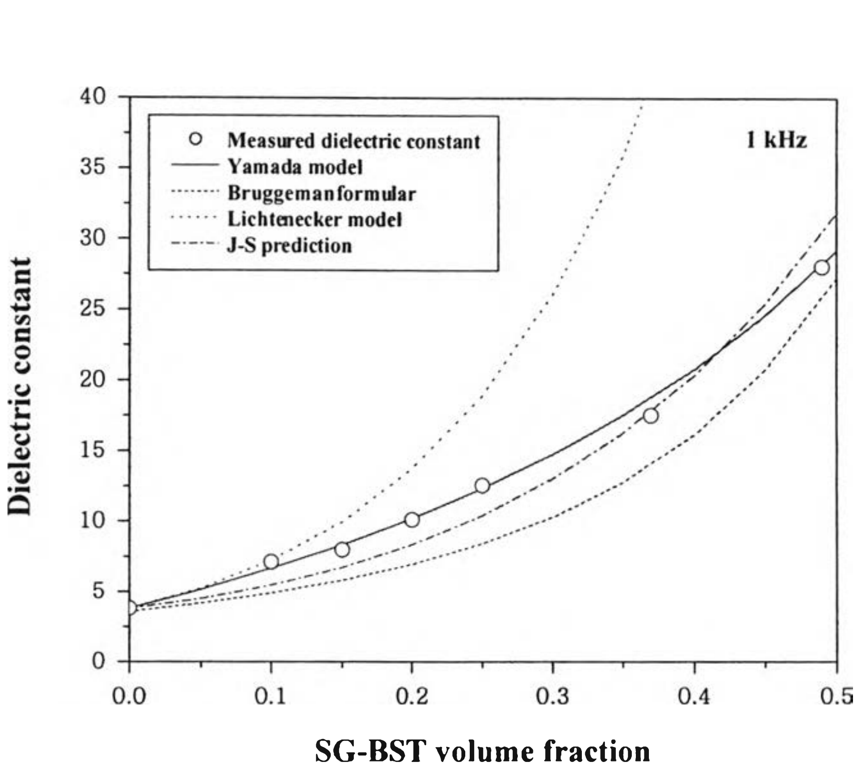

Figure 6.16 Plot of theoretical models and the measured dielectric constant for different SG-BST volume fractions at room temperature and 1 kHz.

From the comparison between the measured dielectric constants and theoretical models, it can be seen from Figure 6.16 that the measured dielectric constants of the SG-BST/polybenzoxazine composites are higher than those calculated from Bruggeman formula and J-S prediction. While the value calculated from Lichtenecker model was higher than the measured dielectric constants. Among these theoretical models, the measured dielectric constants agree quite well with the theoretical prediction based on Yamada model indicating 0-3 connectivity. The shape parameter obtained from fitting Yamada model with experimental data was 6.8, which was an ellipsoid shape (Appendix E). However, Yamada model does not consider the effect of filler agglomeration.

6.5 Conclusions

The dielectric constant of the composites was influenced by ceramic volume fraction. Ceramic powders produced the enhancement of dielectric constant and had more influence on the composite with high ceramic volume fraction. By incorporating 80 wt% (48 vol%) of SG-BST, the dielectric constant was as high as 28. It was about seven times of 3.8 for pure polybenzoxazine at 1kHz. These composites have stable dielectric constants in the frequency range of 1 kHz to 10 MHz. The positive temperature coefficient (PTC) of dielectric constant was nearly zero in the temperature range of 20-130°C, which indicated the low relaxation behavior. Yamada model could fit the measured dielectric constant well for all composites indicating 0-3 connectivity.

6.6 Acknowledgements

The authors wish to thank Dr. Pitak Laoratanakul and MTEC staffs for useful assistance and instrument for characterizations. Also, it was achieved thanks to research grants from the Government Research Budget Year 2005 and Petroleum and Petrochemical College; the National Excellence Center for Petroleum, Petrochemical , and Advanced Materials, Thailand.

6.7 References

[1] S.D. Cho, J.Y. Lee, J.G. Hyun, and K.W. Paik, "Study of epoxy/$BaTiO_3$ composite embedded capacitor films (ECFs) for organic substrate application," *Material Science and Engineering B*, vol. 110, pp. 223-239, 2004.

[2] Y. Rao, S. Ogitani, P. Kohl, and C. P. Wong, "Novel polymer-ceramic nanocomposite based on high dielectric constant epoxy formula for embedded capacitor application," *Journal of Applied Polymer Science*, vol. 83, pp. 1084-1090, 2002.

[3] J. Xu and C.P. Wong, "Effect of the polymer matrices on the dielectric behavior of a percolative high-k polymer composite for embedded capacitor applications," *Journal of Electronic Materials*, vol. 35(5), pp. 1087-1092, 2006.

[4] Y. Rao and C. P. Wong, "Material characterization of a high-dielectric constant polymer-ceramic composite for embedded capacitor applications," *Journal of Applied Polymer Science*, vol. 92, pp. 2228-2231, 2004.

[5] N. G. Devaraju, E. S. Kim, and B. I. Lee, "The synthesis and dielectric study of $BaTiO_3$/polyimide nanocomposite films," *Microelectronic Engineering*, vol. 82, pp. 71-83, 2005.

[6] C.J. Dias and D.K. Das-Gupta, "Inorganic Ceramic/polymer Ferroelectric Composite Electrets," *IEEE Transaction on Dielectric and Electrical Insulation*, vol. 3(5), pp. 706-734, 1996.

[7] L. Ramajo, M. Reboredo, and M. Castro, "Dielectric response and relaxation phenomena in composites of epoxy resin with $BaTiO_3$ particle," *Composites: Part A*, vol. 36, pp. 1267-1274, 2005.

[8] K. Kinoshita and A. Yamaji, "Grain-size effects on dielectric properties in barium titanate ceramics," *Journal of Applied Physics*, vol. 47, pp. 371-376, 1976.

[9] W.R. Buessem, L.E. Cross, and A.K. Goswami, "Phenomenological theory of high permittivity in fine-grained barium titanate," *Journal of the American Ceramic Society*, vol. 49, pp. 33-35, 1966.

[10] M. Klee, "Low-temperature processing of $BaTiO_3$, $BaTi_{1-x}Zr_xO_3$ and $Ba_{1-x}Sr_xTiO_3$ powder," *Journal of Material Science Letters*, vol. 8(8), pp. 985-988, 1989.

[11] N.V. Giridharan, R. Varatharajan, R. Jayavel, and P. Ramasamy, "Fabrication and characterization of $(Ba,Sr)TiO_3$ thin film by sol-gel technique through organic precursor route," *Materials Chemistry and Physics*, vol. 65, pp. 261-265, 2000.

[12] C. Fu, C. Yang, H. Chen, Y. Wang, and L. Hu, "Microstructure and dielectric properties of $Ba_xSr_{1-x}TiO_3$ ceramics," *Materials Science and Engineering B*, vol. 119, pp. 185-188, 2005.

[13] W. Yang, A. Chang, and B. Yang, "Preparation of barium strontium titanate ceramic by sol-gel method and microwave sintering," *Journal of Materials Synthesis and Processing*, vol. 10 (6), pp. 303-309, 2003.

[14] S.B. Shen and H. Ishida, "Dynamic mechanical and thermal characterization of high-performance polybenzoxazine," *Journal of Polymer Science Part B: Polymer Physics*, vol. 37, pp. 3257-3268, 1999.

[15] T. Yamada, T. Ueda, and T. Kitayama, "Piezoelectricity of a high–content lead zirconate titanate/polymer composite," *Journal of Applied Physics*, vol. 53(6), pp. 4328-4332. 1982.

[16] N.E. Frost, P.B. McGrath, and C.W. Burns, "Effect of fillers on the dielectric properties of polymers," *IEEE International Symposium on Electrical Insulation*, pp. 300-303, 1996.

[17] N. Jayasundere and B.V. Smith, "Dielectric constant for binary piezoelectric 0-3 composites," *Journal of Applied physics*, 73 (5), 2462-2466. 1993.

[18] D.J. Allen and H. Ishida, "Physical and mechanical properties of flexible polybenzoxazine resins: effect of aliphatic diamine chain length," *Journal of Applied Polymer Science*, vol. 101, pp. 2798-2809, 2006.

[19] D.H. Kuo, C.C. Chang, T.Y. Su, W.K. Wang, and B.Y. Lin, "Dielectric behaviours of multi-doped $BaTiO_3$/epoxy composites," *Journal of the European Ceramic Society*, vol. 21, pp. 1171-1177, 2001.

[20] H.C. Pant, M.K. Patra, A. Verma, S.R. Vadera, and N. Kumar, "Study of the properties of barium titanate-polymer composites," *Acta Material*, vol. 54, pp. 3163-3169, 2006.

[21] S.H. Xie, B.K. Zhu, X.Z. Wei, Z.K. Xu, and Y.Y. Xu, "Polyimide/$BaTiO_3$ composite with controllable dielectric properties," *Composite: Part A*, vol. 36, pp. 1152-1157, 2004.

[22] K.C. Cheng, C.M. Lin, S.F. Wang, S.T. Lin, C.F. Yang, "Dielectric properties of epoxy resin-barium titanate composites at high frequency" *Materials Letters*, vol. 61(3), pp. 757-760, 2007.